Cerebral Cortex Advance Access published August 11, 2011

Cerebral Cortex
doi:10.1093/cercor/bhr191

Heterogeneous Spine Loss in Layer 5 Cortical Neurons after Spinal Cord Injury

Arko Ghosh[1,2], Stefano Peduzzi[1], Moina Snyder[1], Regula Schneider[1], Michelle Starkey and Martin E. Schwab[1]

[1]Brain Research Institute and [2]Institute of Neuroinformatics, University of Zurich and Swiss Federal Institute of Technology (ETH), 8057 Zurich, Switzerland

Address correspondence to Arko Ghosh, Institute of Neuroinformatics, University of Zurich and Swiss Federal Institute of Technology (ETH) Winterthurerstrasse 190, 8057 Zurich, Switzerland. Email: arko@ini.phys.ethz.ch.

A large thoracic spinal cord injury disconnects the hindlimb (HL) sensory-motor cortex from its target, the lumbar spinal cord. The fate of the synaptic structures of the axotomized cortical neurons is not well studied. We evaluated the density of spines on axotomized corticospinal neurons at 3, 7, and 21 days after the injury in adult mice expressing yellow fluorescence protein in a subset of layer 5 neurons. Spine density of the dendritic segment proximal to the soma (in layer 5) declined as early as 3 days after injury, far preceding the onset of somatic atrophy. In the distal segment (in layer 2/3), spine loss was slower and less severe than in the proximal segment. Axotomy of corticospinal axons in the brainstem (pyramidotomy) induced a comparable reduction of spine density, demonstrating that the loss is not restricted to the neurons axotomized in the thoracic spinal cord. Surprisingly, in both forms of injury, the spine density of putative non-axotomized layer 5 neurons was reduced as well. The spine loss may reflect fast rearrangements of cortical circuits after axotomy, for example, by a disconnection of HL cortical neurons from synaptic inputs that no longer provide useful information.

Keywords: cortical plasticity, corticospinal, dendritic spine, spinal cord injury, synapses

Introduction

A thoracic spinal cord bilateral dorsal hemisection transects the main corticospinal tract (CST) and the ascending dorsal column pathways, resulting in dysfunctional hindlimbs (HLs). The HL sensory-motor cortex is deprived of the touch and proprioceptive information from the HLs (Asanuma and Arissian 1982; Kaas et al. 2008), and the corticospinal neurons cannot deliver their output. Within 7 days after bilateral dorsal hemisection in adult rats, the forelimb sensory representation enlarges and invades the HL area (Ghosh et al. 2010). Axotomized corticospinal neurons can survive the injury but become atrophic after 2–4 weeks (Barron et al. 1988; Merline and Kalil 1990; Wannier et al. 2005; Carter et al. 2008) and whether all the corticospinal neurons survive is contentious (Hains et al. 2003; Nielson et al. 2010). Nevertheless, the role of the injured neurons in the CNS remains largely unclear, but some of the neurons were shown to contact new targets and assume novel functions to control the injury-spared body parts (Fouad et al. 2001; Bareyre et al. 2004; Ghosh et al. 2010). How the axotomy influences the synaptic structures of the lesioned corticospinal neurons has not been explored.

The large dendritic trees of corticospinal neurons, like other layer 5 pyramidal neurons, are endowed with spines that receive most of the excitatory inputs. The dendrites traverse through and make synapses in the more superficial layers and also in layer 5. The presence, number, and shape of spines can be used as an indicator of synaptic changes (Yuste and Bonhoeffer 2001; Fiala et al. 2002). Interestingly, after a spinal cord injury that interrupts both sensory and motor pathways in mice, a transitory reduction in spine density has been reported in layer 5/6 cells of the motor cortex, but the quantifications were restricted to the basal dendrites which largely project in the same layer (Kim et al. 2006). This may not reflect the true changes in the corticospinal cells as they make up only about 25% of the layer 5 population (McComas and Wilson 1968; Akintunde and Buxton 1992; Kaneko et al. 2000). Furthermore, it is not known whether the change in spine density of the dendrites in layer 5 differs from the dendrites located in the more superficial layers.

In this study, we determined the dendritic spine density from a subset of layer 5 neurons along the entire 420-μm-long apical dendrite traveling through cortical layers 5 to 2/3. We focused on the HL sensory-motor cortex in mice before and 3, 7, and 21 days after thoracic spinal cord injury. By using retrograde labeling from the injury site, axotomized and putative non-axotomsied cortical neurons were identified in the adult animals expressing yellow fluorescence protein (YFP) in layer 5 neurons (Feng et al. 2000). The YFP allowed for a "Golgi-like" visualization of the dendritic tree and the synaptic structures. Our findings show that several factors influence the loss of dendritic spines: the state of the axon, the location of the cell in the HL field, and the layer in which the dendritic region resides. Importantly, spine loss also occurred on the neighboring putative intact neurons, possibly reflecting major changes in intracortical connectivity. By using CST lesion at the brain stem (pyramidotomy), we show that the spines are as vulnerable when the axons are injured closer to the soma. Taken together, our results show that the axotomy of corticospinal neurons induces spine loss in the sensory-motor cortex, in both the injured and putative intact layer 5 projection neurons. These changes may lead to the disconnection of cortical output neurons from the injury-inflicted network.

Materials and Methods

Animals

Founders of our colony of transgenic mice expressing the YFP transgene driven by thy1 promoter were obtained from Jackson Labs (Bar Harbor, ME). Twenty-one adult (6–7 weeks old) C57BL/6 thy1-YFP (line H) heterozygous female mice were used in this study (Feng et al. 2000). Animals were housed in small groups (3–5) and in female-only cages after weaning. The cages were individually ventilated and covered with a filter top. All experimental procedures performed were in adherence to the guidelines of the Veterinary office of the Canton of Zurich, Switzerland.

Spinal Cord Injury and Pyramidotomy

Mice were anesthetized by an intraperitoneal injection of Hypnorm (Jansen Pharmaceutica, Beerse, Belgium) and Dormicom (Roche

Pharma, Basel, Switzerland). A partial lamenectomy was performed at the thoracic level T8. Using a sharp iridectomy scissors, the dorsal half of the spinal cord was transected (bilaterally) including the dorsal and the dorsolateral funiculi and the dorsal horn. For unilateral pyramidotomy, the medulla was reached by a ventral approach (Starkey et al. 2005) and the pyramidal tract was cut under the guidance of epifluorescence goggles. The retrograde tracer Fast Blue (1%, suspension in 0.1 M phosphate buffer and 2% dimethyl sulfoxide, EMS-Polyloy, GrossUmstadt, Germany) was placed at the lesion sites for 15 min. Excess dye was removed using a cotton sphere. All animals were perfused with phosphate-buffered saline followed by 4% paraformaldehyde. The cortices were sucrose treated, frozen, and cut into 75-μm-thick coronal slices (cross sections) on a cryostat. The brainstem and spinal cord were similarly processed to examine the lesion sites (for lesions, see Supplementary Fig.).

Imaging—Spine Count and Soma Volume

Images were acquired using a confocal microscope (Leica DM16000, CLSM-Model SP5). The excitation wavelengths were 405 and 488 nm, for Fast Blue and YFP, respectively. Cells of interest were identified on 512 × 512 pixel images (pixel size: 283.22 × 283.22 nm) and spines were quantified on 1024 × 1024 pixel images (pixel size: 141.47 × 141.47 nm, *Z*-step 136.0 nm). Spines were marked using Image J running the View5D plug-in (Rainer Heintzmann, King's College London, London, UK). A custom-written Matlab (MathWorks, Princeton, NJ) script was used to reconstruct the data from multiple cross sections. This plug-in allowed us to view the spines in 3D and the background in the gray images was set at 15 (on a 255 scale—8 bit). A maximum of 5 and a minimum of 4 markers were used to describe each spine; one placed at the base, one on the tip, one at the point of bending (when the spine appeared bent), and 2 on the spine head capturing its width (see Supplementary Fig.). The distance of the spine from the soma was calculated in 3D using the markers placed at the base of the spine; the markers were used to construct a stick figure of the dendrite from each cross section (see Supplementary Fig.)—several stick figures belonging to the same dendrite were connected to reconstruct 420-μm-long segments. The diameter of the dendrite was measured at a distance of 30 μm from the soma using 2 markers; placed on the cross section to span the diameter. All spines and dendrites were measured by an observer (SP) blind to the experimental conditions.

For volume measurements, the cell body was reconstructed in 3D using Imaris (Bitplane AG, Zurich, Switzerland)—based on the YFP signal—and the soma volume was estimated using Imaris MeasurementPro (Bitplane AG, Zurich, Switzerland) from the generated isosurface. The soma was cropped in 3D to exclude the basal and apical dendrites and the axon. Forty neurons—belonging to intact and spinal cord injured conditions (10 per group)—were selected for these measurements. Cells were selected such that the entire soma was within a single 75-μm-thick coronal section.

Cell Selection

Axotomized YFP^+ neurons were selected for the spine counts based on the following: 1) soma well filled with Fast Blue were preferred over neurons with patchy filling and 2) only cells with apical dendrite that could be followed through 2 or more brain slices (upto 420 μm distal to the soma) were considered. Putative non-axotomized cells were similarly selected, except that they were Fast $Blue^-$. Thus, we identified and studied the 2 groups of cells 1) YFP^+ and Fast $Blue^+$—axotomized neurons and 2) YFP^+ and Fast $Blue^-$—Putative non-axotomized neurons. A third cell group was Fast $Blue^+$ only (axotomized but YFP^-) and it was not considered for the measurements. Neurons belonging to each experimental condition (n = 10 cells per group except in the non-axotomized 7 days after spinal cord injury group where n = 20) were from at least 3 animals (see Supplementary Table). For instance, in the control condition, the 10 rostral neurons were from 3 animals—with 2 animals contributing to 3 cells each and 4 neurons were gathered from one animal.

The HL corticospinal maps derived from the spinal cord–injured animals at 7 and 21 days after injury were used to define the rostral and central HL regions in all the animals. The maps were constructed based on the Fast $Blue^+$ cell positions relative to bregma, and the cells were marked using the software Neurolucida (MicroBrightField, Williston, VT) mounted on a conventional fluorescence microscope. The rostral cells originated in front of the bregma and were from an area enclosed in a 0.2 mm radius semicircle drawn at *X*: 1.2 mm (lateral to bregma) and *Y*: 0 mm (from the bregma line). The central cells were selected from an area enclosed in a 0.2 mm radius circle drawn at *X*: 1.1 mm and Y:–0.6 mm.

Statistical Analysis

Our data set did not allow us to assume normal distribution and therefore nonparamatric statistical tests were used. Data sets consisting of more than 2 groups were first evaluated using the Kruskal–Wallis nonparametric analysis of variance followed by the pairwise Mann–Whitney test. When comparing 2 groups, the Mann–Whitney test alone was used. The threshold P value was 0.05 in all the tests.

Results

Retrograde Identification of Axotomized Corticospinal Neurons

We retrogradely labeled axotomized corticospinal neurons from the site of axonal injury with the tracer Fast Blue in thy1-YFP mice (Line H). The dye was applied at the time of the axonal injury in the cord or brain stem. YFP expression was limited to cortical layer 5b—the deeper sublayer of layer 5 (Fig. 1*A*, insert); about 25% of the retrogradely labeled cells in the HL sensory-motor cortex expressed YFP. Moreover, nontufted neurons were not visible suggesting that the vast majority of the callosal neurons originating from layer 5 do not express YFP (Hubener and Bolz 1988; Supplementary Fig.). Importantly, callosal cells do not project to the spinal cord (Catsman-Berrevoets et al. 1980) and as corticospinal neurons originate from layer 5b, the Line H mice were suitable for our study. After a bilateral dorsal hemisection of the thoracic spinal cord, the HL field was mapped by reconstruction of the positions of the retrogradely labeled cells in the sensory-motor cortex (Fig. 1*B*).

Three different cell types were identified in the injured animals 1) putatively intact and not a corticospinal neuron—Fast $Blue^-$ and YFP^+, 2) axotomized corticospinal neuron—Fast $Blue^+$ and YFP^-, and 3) axotomized corticospinal neurons with visible morphology—Fast $Blue^+$ and YFP^+ (Fig. 1*C*). The morphology was evaluated only in the neurons belonging to category "1" and "3" as the YFP was expressed in the entire cell and Fast Blue filled primarily the soma. A fourth category of cells, intact neuron, and Fast $Blue^+$ may be ruled out as there was no evidence of cells labeled in the forelimb cortex—which would have resulted from the dye diffusing into the higher spinal segments to label the intact neurons. Moreover, using Fast Blue, it was not possible to label intact corticospinal axons passing through the densely packed dorsal funiculus by topical application alone. This is in agreement with the general notion that retrograde tracer uptake is enhanced by axonal injury in the CNS (see Discussion on the notion in Haase and Payne 1990).

We cannot be certain that the Fast $Blue^-$ neurons are in fact all intact (hence termed as putatively intact) as the retrograde tracer is not expected to label 100% of the axotomized cells. According to the cell counts, 3 days after pyramidotomy, 43% of YFP^+ neurons from the center of the HL sensory-motor cortex were retrogradely labeled (Fig. 1*D*) and YFP is presumably expressed in a random selection of layer 5b neurons. Considering the YFP^+ neurons to be representative of the

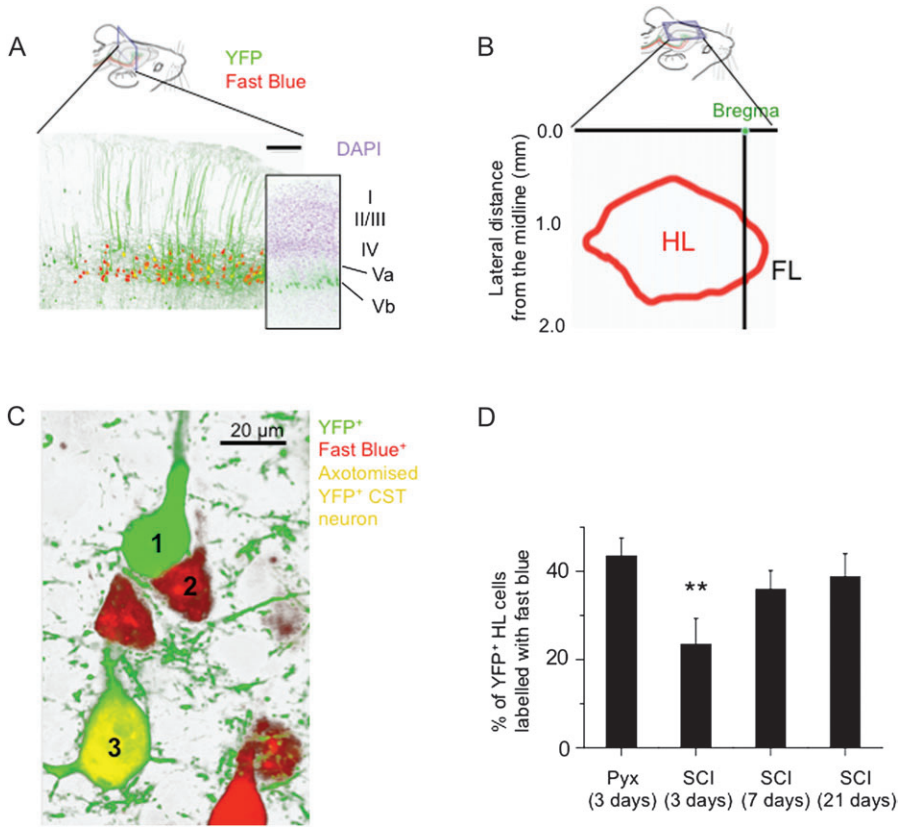

Figure 1. Retrograde identification of axotomized neurons in thy1-YFP mice. (*A*) A 15-µm-thick confocal section showing YFP-expressing layer 5b neurons (green) and Fast Blue (red) positive corticospinal cell bodies labeled from the site of injury in the thoracic spinal cord. Scale bar, 100 µm. Insert, DAPI nuclear staining of the sensory-motor cortex reveals that YFP^+ cells are exclusively located in layer 5b. (*B*) Mapping the positions of 1541 HL corticospinal neurons (from every second 75-µm brain slice). HL, hindlimb corticospinal field; FL, forelimb field. (*C*) We identified putative non-axotomized YFP^+ cells (1), cells labeled only with Fast Blue, that is, axotomized but not YFP^+ cells (2) and double labeled, that is, axotomized YFP^+ cells (3). (*D*) Percentage double-labeled cells of the HL YFP^+ population after spinal cord injury (SCI) and pyramidotomy (Pyx); based on three 75-µm-thick sections per animal, $n = 3$ mice. Error bars represent ± SEM. Data were subjected to Mann–Whitney test compared with the pyramidotomy condition. $^{**}P < 0.01$.

entire layer 5b population, we estimate that 43% of layer 5b neurons in the HL area are corticospinal. Seven days of survival after the tracer injection was required to obtain a maximal number of labeled cells after a thoracic spinal cord injury (Fig. 1*D*). Remarkably, a previous report found that 50% of the layer 5b Nissl-stained neurons were retrogradely labeled from the spinal cord (Kaneko et al. 2000); in the report, the authors do not mention 5b but their sample only included the Nissl-stained neurons "in the vicinity of" the retrogadely labeled cells and corticospinal neurons project only from layer 5b. Another older study estimated labeled corticospinal neurons constitute of about 23% of the neurons projecting to subcortical targets mainly from layer 5 (Akintunde and Buxton 1992). Moreover, in an electrophysiological study, 31% of the neurons encountered at depths between 0.9 and 1.3 mm—presumably layer 5—were identified as pyramidal tract neurons (McComas and Wilson 1968). The 2 later studies do not reveal what proportion of layer 5b neurons are corticospinal, but as the size of 5a is roughly similar to 5b (Fig. 1*A*, insert), about 50–60% of the 5b neurons must be corticospinal. Taken together, we suggest that we were able to label and detect axotomized corticospinal cells using Fast Blue with a close to 80% certainty; this also implies that the likelihood of $Fast\ Blue^-$ neurons being intact is very high.

One reason for the better than expected rate of retrograde identification could be laser scanning confocal microscopy as it is more efficient in detecting labeled cells than conventional fluorescence microscopy. For example, cell counts from a 75-µm-thick section revealed 202 cells after confocal imaging compared with just 67 cells using the conventional microscope.

Dendritic Spine Density in Intact Animals

We assessed the synapse density in the HL sensory-motor cortex along the apical dendritic trunk of layer 5b neurons as they passed through layer 5a to reach layer 2/3 (Fig. 2). In intact animals, we selected 10 YFP^+ pyramidal cells from the center of the HLfield (Fig. 2*A*,*B*) and 10 HL cells that were located in the rostral rim (Fig. 2*C*), in proximity to the forelimb (FL) area; in mice and rats, the FL area mainly lies rostral to the HL area (Ayling et al. 2009; Brown et al. 2009; Ghosh et al. 2009). In all the neurons, spines were rarely observed on the apical dendrite close to the soma—in the first 30 µm—and in the next 40 µm, the density was low (rostral rim cells, median of 0.6 spine/µm ±0.09 standard error of the mean [SEM]; center cells, 0.5 spine/µm ±0.10 SEM). Spine density increased by approximately 3-fold (rostral cells, 1.7 spine/µm ±0.06 SEM; center cells, 2.1 spines/µm ±0.10 SEM) as the dendrite traveled through layer 5a (130–210 µm from the soma, referred to as the proximal segment in Fig. 2*E*). Compared with the proximal segment, the spine densities were about 1.5-fold less on the dendrite passing through layer 2/3 at 330–410 µm from the soma (referred to as the distal segment in Fig. 2*D*, rostral cells,

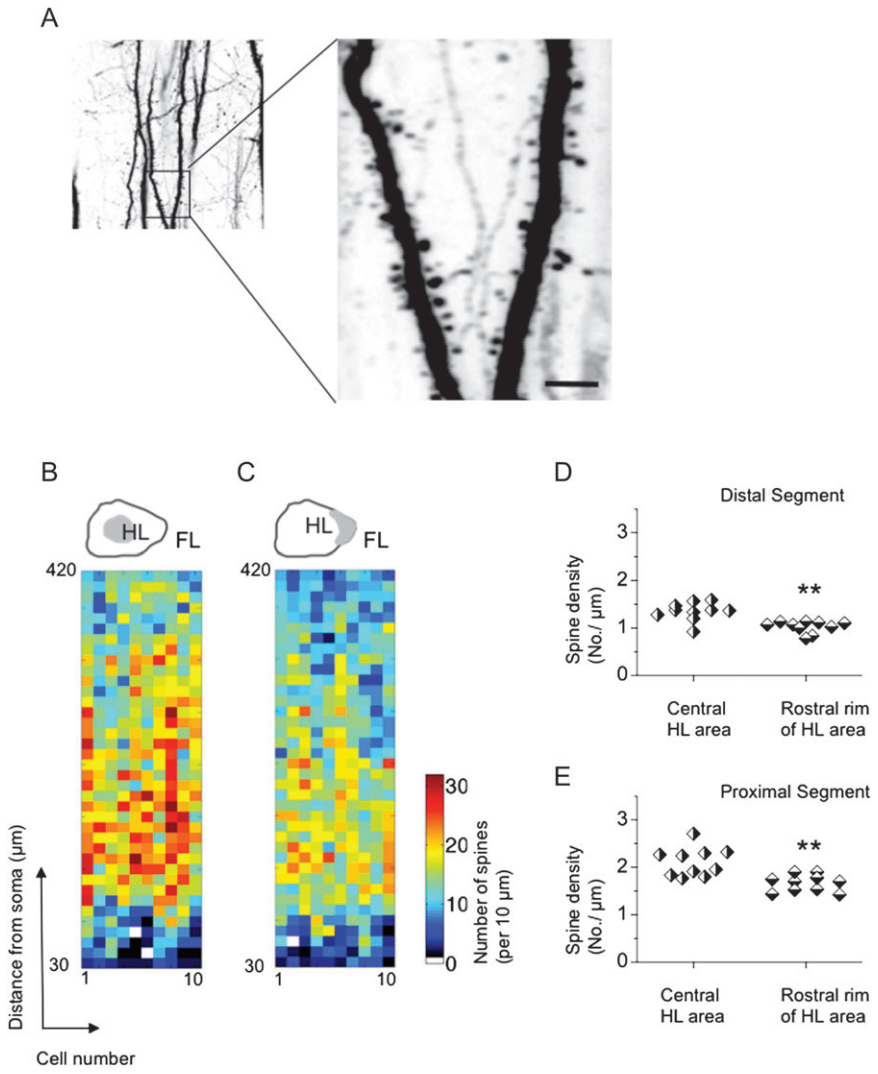

Figure 2. Spine density on the apical dendrites of the HL sensory-motor cortex in intact animals. (*A*) In the thy1-YFP mouse, spines could be easily visualized by confocal microscopy. Scale bar, 5 μm. (*B*,*C*) Spine density profile along the apical dendrite in 10 layer 5b neurons from the center (shaded area, B) or the rostral rim (*C*) of the HL field. A column depicts a single neuron. (*D*,*E*) Spine density distribution in the proximal (130–210 μm from the soma, (*E*) or distal (330–410 μm from the soma, (*D*) segment of apical dendrites. Statistics as in previous figure, $n = 10$ neurons.

1.1 spine/μm ±0.04 SEM; center cells, 1.4 spine/μm ±0.06 SEM). Notably, in both proximal and distal segments, cells located in the rostral rim had fewer spines (Fig. 2*B–E*). We would like to stress here that there was no retrograde labeling from the spinal cord in the intact animals and there is about a 45% possibility for each neuron to be corticospinal.

Loss of Dendritic Spines in the HL Cortex after Spinal Cord Injury

To determine the changes in spine density after spinal cord injury, we compared the axotomized corticospinal neurons to the cells evaluated in the intact mice (Fig. 3). At 3 days after thoracic spinal cord injury, in the center of the HL field, there was a small but significant loss of spine density on the proximal dendritic segments of the axotomized neurons (Fig. 3*B*,*F*). At 7 days, however, spine density was strongly reduced by about 50% (1.1 spine/μm ±0.09 SEM compared with 2.1 spine/μm ±0.10 SEM in intact animals; Fig. 3*C*,*F*). The density remained low at 21 days after injury (Fig. 3*D*,*F*). In the distal segment, spine loss was less drastic (Fig. 3*B–E*). At 21 days after injury, spine densities were reduced by about 40% (0.9 spine/μm ±0.09 SEM compared with 1.4 spine/μm ±0.06 SEM in intact animals).

The detailed analysis done in this study allowed us to search for correlations on the single cell level. Interestingly, the loss of spine was not uniform along the length of the same dendrite: There was no significant relationship between the spine densities in the proximal and distal segments at any time point after injury (at 3 days, $r^2 = -0.07$ $P = 0.85$; at 7 days, $r^2 = 0.39$ $P = 0.26$; at 21 days, $r^2 = 0.36$ $P = 0.31$). In agreement to previous studies, we found no loss in the somatic volume of axotomized neurons at 3 or 7 days after the injury (Ganchrow and Bernstein 1981; Barron et al. 1988). The median cell body volume of axotomized CST neurons dropped from 2800 μm^3 ±280 SEM in intact animals to 1963 μm^3 ±212 SEM at 21 days after injury ($n = 10$ neurons). We also addressed whether the atrophied cells carried fewer spines and found no significant correlation between the proximal dendritic segment's spine density and the somatic volume ($r^2 = -0.36$ $P = 0.15$, at 21 days $n = 10$).

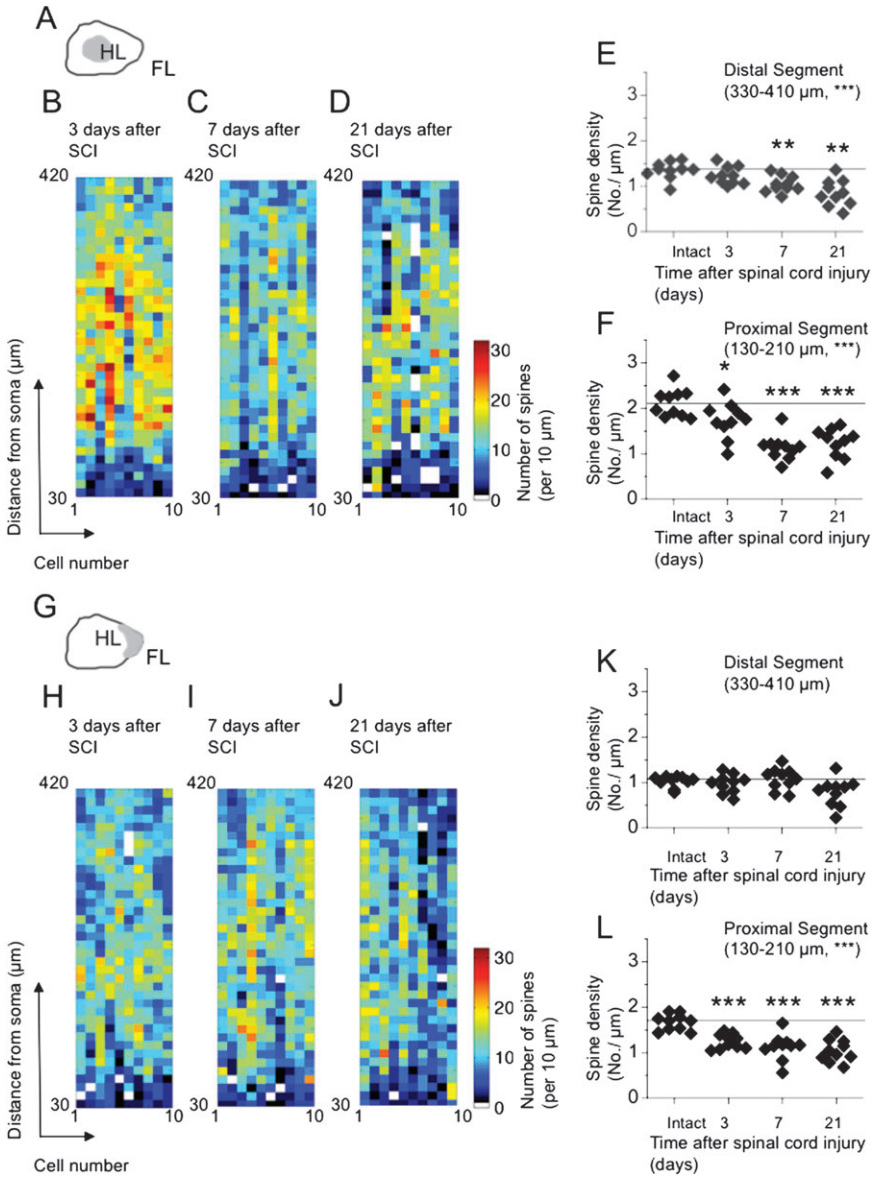

Figure 3. Spine density of axotomized corticospinal neuron apical dendrites after a thoracic spinal cord injury. (*A*) Location (shaded area) from which the cells in *B–F* were selected. (*B–D*) Spine density profiles 3 (*B*), 7 (*C*), or 21 (*D*) days after spinal cord injury along the apical dendrite. (*E,F*) Distribution of spine densities in the proximal (*F*) or distal (*E*) segments of the apical dendrite. Solid line shows the median spine density of YFP^{+} (layer 5b) population in intact animals. (*G*) Location of the rostral rim in the HL field (shaded area) from which cells were selected for *H* to *L*. (*H–J*) Color profiles of spine density 3 (*H*), 7 (*I*), or 21 (*J*) days after spinal cord injury along the apical dendrite. (*K–L*) Distribution of spine densities in proximal (*L*) or distal (*K*) segments of the apical dendrites. $n = 10$ cells selected from at least 3 mice per group. Data were subjected first to Kruskal–Wallis analysis of variance followed by Mann–Whitney test compared with the intact group. The analysis of variance results are depicted in brackets on the right corner of every graph and Mann–Whitney test on the top of each group. $^{*}P < 0.05$, $^{**}P < 0.01$, $^{***}P < 0.001$.

Axotomized HL neurons located in the rostral rim of the HL field (Fig. 3*G–L*) showed a consistent spine loss in the proximal segment starting at 3 days after injury (1.2 spine/μm ±0.05 SEM compared with 1.7 spine/μm ±0.06 SEM in intact mice). In contrast to the cells in the center of the HL field, the distal segment of rostral rim neurons revealed no significant reduction in spine density after injury (Fig. 3*K*). In summary, in the HL CST axotomized neurons, the spine loss was more drastic in the proximal dendritic segment than in the distal segment and spine loss in the distal segment was attenuated at the rostral rim of the HL cortex.

We restricted our analysis of the putative non-axotomized neurons to 7 and 21 days after injury (Fig. 4*A–E*); at these time points due to the large proportion of layer 5b neurons that were retrogradely labeled, it was safer to assume that neurons without Fast Blue were non-axotomized. At 7 days, the spine densities on the proximal segments of the center field neurons were reduced (Fig. 4*B,E*); however, this reduction was less than in axotomized neurons (1.5 spine/μm ±0.06 SEM in non-axotomized neurons compared with 1.1 spine/μm ±0.09 SEM in axotomized neurons, $P < 0.001$). There was no significant reduction in spine density on the distal segments (Fig. 4*D*). At 21 days, the proximal segments of the putative non-axotomized neurons showed reduced spine density (Fig. 4*C–E*), however, less drastic than in axotomized neurons (proximal segment, 1.5 spine/μm ±0.08 SEM in putative

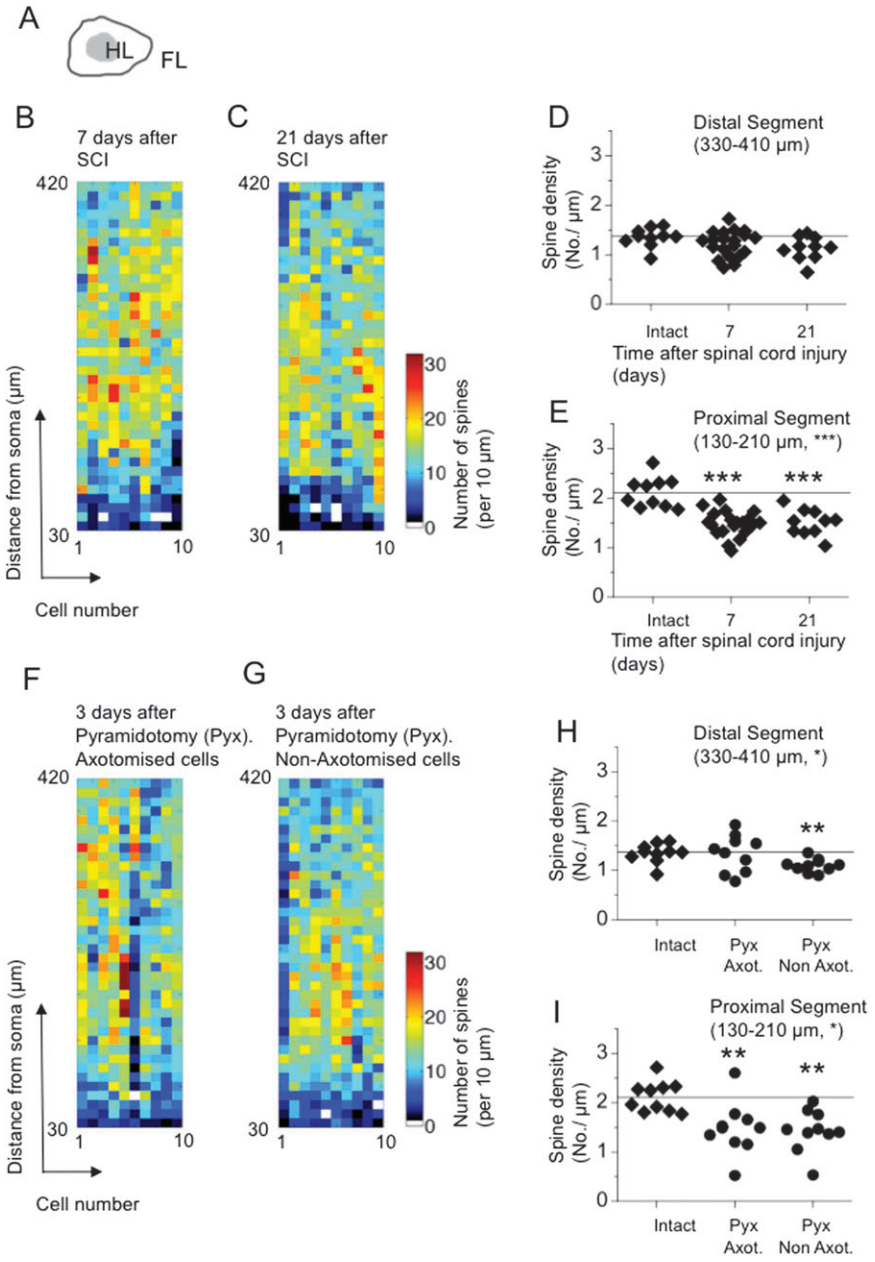

Figure 4. Spine density of putative non-axotomized neurons after spinal cord injury or pyramidotomy. (*A*) Scheme showing location of the HL field (in gray) from which cells in *B–I* were chosen. *B–C* Spine density 7 (*B*) or 21 (*C*) days after spinal cord injury along the apical dendrite in putative non-axotomized neurons. (*D,E*): Distribution of spine densities in proximal (*E*) or distal (*D*) segments of the apical dendrite in putatively non-axotomized neurons. (*F,G*) Spine density of axotomized (*F*) or putative non-axotomized (*G*) neurons in the center of the HL field 3 days after pyramidotomy. (*H–I*) Distribution of spine densities in the proximal (*I*) or distal (*H*) segment of the apical dendrite in axotomized (Axot.) and putative non-axotomized (Non-axot.) neurons after pyramidotomy. Statistics as in Figure 3, except ($n = 20$) cells at the day 7 time point in *D* and *E*.

non-axotomized neurons compared with 1.2 spine/μm ±0.1 SEM in axotomized neurons, $P < 0.05$).

Loss of Spines after Selective Axotomy of Corticospinal Neurons in the Pyramid

We performed a unilateral pyramidotomy, which transects majority (~95%) of the CST neurons projecting to the hemicord at the level of the brain stem (Brosamle and Schwab 1997; Fig. 4*F–I*). Spine loss occurred at 3 days after pyramidotomy in the proximal segment of both axotomized and putative non-axotomized neurons (1.5 spine/μm ±0.17 SEM in axotomized neurons, 1.4 spine/μm ±0.13 SEM in non-axotomized compared with 2.1 spine/μm in intact animals). The loss of spine in the proximal segment of the axotomized neurons was similar to spinal cord injury (1.7 spine/μm ±0.13 SEM at 3 days after spinal cord injury) and the distal spines were not significantly influenced at this time point. These results show that the vulnerability of the proximal spines and the preservation of the distal spines are not unique to spinal cord injury and that a similar pattern can be induced by an injury at a much higher level. Interestingly, the distal spine density of the putatively non-axotomized population was reduced after pyramidotomy (1.1 spine/μm ±0.04 SEM compared with 1.4 spine/μm ±0.06 SEM in intact animals).

Discussion

To address the synaptic alterations in corticospinal neurons after spinal cord injury, we took advantage of retrograde labeling from the thoracic spinal cord lesion site in a transgenic mouse line that allowed a Golgi-like visualization of layer 5b pyramidal neurons. Spine loss was unequal among the analyzed neuronal sample, more pronounced on the proximal part of the apical dendrites, and larger in the center of the HLfield. A comparable spine loss was also present in the putative non-axotomsied neurons and upon lesion of the corticospinal neurons in the brainstem (pyramidotomy). The synaptic loss after spinal cord injury may be a key event for rewiring the dysfunctional cortical circuits and the vulnerability of the proximal spines is not restricted to the neurons axotomized in the thoracic spinal cord.

YFP^+ neurons without the retrograde label Fast Blue were identified as putative non-axotomized neurons in the injured mice. The following observations rule out that there were a significant number of unlabelled axotomized neurons due to the lack of tracer uptake: Confocal imaging was able to detect cell bodies sparsely filled with the retrograde tracer that were invisible in a conventional fluorescent microscope. Therefore, the described inefficiency of retrograde labeling is certainly less when using confocal imaging. Confocal imaging has been previously used to detect retrogradely labeled corticospinal neurons with a similar, higher than expected, efficiency (Kaneko et al. 2000). About 40% of YFP^+ cells were retrogradely labeled from the spinal injury site, close to the estimate of the proportion of corticospinal neurons in a population of Nissl-stained layer 5b population (Kaneko et al. 2000). Moreover, the extent, location, and time course of spine loss was distinct in the population of neurons that we identified as putatively non-axotomized compared with the axotomized population. For example, at 7 days after spinal cord injury, the spine loss on the proximal segments was significantly lower in the putative non-axotomized neurons than in the axotomized cells.

To assess injury-induced synaptic alterations, we compared the spine densities on the axotomized corticospinal neurons—identified using Fast Blue—in the injured groups to the layer 5b YFP^+ neurons in intact animals. In the intact group, the layer 5b population probably consisted of neurons projecting to the midbrain, pons, and medulla oblongata, in addition to the spinal cord–projecting neurons. This raises the possibility that our comparisons in part reflect different cell populations rather than the impact of axonal injury. The similarities between the spine density profiles in the center of the HL field in intact animals and in axotomized corticospinal neurons 3 days after spinal cord injury, when spine loss was still low (proximal segment) or absent (distal segment), do not support the notion that dendritic spine density is dramatically distinct in corticospinal neurons. Our claim of spine loss after spinal cord injury is strengthened by the observation that spine density in the retrogradely labeled neurons is lesser at 7 or 21 days than at 3 days after injury—in this case, the comparison is between corticospinal neurons.

In our study, we did not find a correlation between spine loss and somatic atrophy in axotomized neurons at 21 days after injury, albeit our finding is from 10 neurons. The distinction between a somatic and a spine pathway is supported by the observation that somatic atrophy is not accompanied by dendritic atrophy in axotomized corticospinal neurons (Tseng and Prince 1996). In optic nerve lesions, the length of the remaining axon is an important factor linked to the likelihood of cell death and expression of growth-related genes (Doster et al. 1991; Wu et al. 2010). However, in our study, we find the proximal and distal spines of axotomized corticospinal neurons to be similarly vulnerable irrespective of the level of injury, that is, at the thoracic spinal cord versus the brain stem. In addition, dendritic spines were lost in the putative non-axotomized neurons after both spinal cord injury and pyramidotomy. Taken together, we suggest that mechanisms not directly related to the axonal injury or axotomy-induced trophic factor loss must be involved, particularly in the non-axotomized population. The differential extent of spine loss on the same apical dendrite in proximal versus distal segments in axotomized and putative non-axotomized neurons after spinal cord injury points toward the involvement of mechanisms that distinctly influence the dendrites dependent on the layer that they pass through. These mechanisms could be cortical activity dependent. In the adult primary sensory cortex, sensory inputs can influence the connectivity at the level of dendritic spines by altering their motility (Trachtenberg et al. 2002; Keck et al. 2008). Moreover, deprivation from sensory inputs results in the reduction of spine density in the whisker barrel and visual cortices (Globus et al. 1973; Kossut 1998). The thoracic spinal cord injury used here results in sensory deprivation due to the transected dorsal funiculus, and a significant loss of sensory fibers cannot be ruled out in neighborhood of the pyramidotomy as shown in Starkey et al. (2005).

The documented spine loss in the injury inflicted HL cortex after thoracic spinal cord injury must be compared with a previous study on the forelimb motor cortex after cervical lesion (Kim et al. 2006). The cervical lesion resulted in a 10% reduction of overall spine density at 7 days the injury determined from short segments of basal dendrites, in both layer 5/6 and layer 3 pyramidal neurons. Axotomized cells were not identified; these constitute a maximum of 15% of the layer 5/6 population. The reduction was transient and by 28 days the spine density recovered to baseline levels. In the present study, we did not observe any recovery of spine density at 21 days after injury, even in the putative non-axotomized neurons. This discrepancy may be due to several reasons that include different classes of dendrites evaluated, sensitivity of the methods, location of the injury, and cortical area of interest. Another reason may be that our examination included specifically layer 5b neurons, whereas the cells evaluated in the previous study could belong to any of the sublayers of layer 5 and layer 6. Nevertheless, both the studies suggest an impact on the neurons that are not axotomized.

How does the spine loss affect the cortical circuitry? It must be noted here that the spine loss detected using fluorescence microscopy is very likely to reflect synaptic loss; this is supported by key experiments that imaged sensory cortical spine loss in vivo using thy1-GFP mice followed by electron microscopy (Trachtenberg et al. 2002). On the other hand, at least some of the spared spines must be functional as axotomized HL corticospinal neurons can respond to forelimb sensory inputs (Ghosh et al. 2010). The layer 5b pyramidal neurons in the injury affected HL cortex had about 20–50% fewer spines at 21 days after thoracic injury than in intact animals. It has been previously shown that by 3–4 weeks after a thoracic spinal cord injury, corticospinal neurons from the

HL sensory-motor cortex can sprout new collaterals into the cervical spinal cord accompanied by the appearance of forelimb movements upon HL cortical stimulation (Fouad et al. 2001; Ghosh et al. 2010). Interestingly, HL corticospinal neurons respond faster to forelimb sensory input at 1 week after thoracic spinal cord injury than in intact animals, even though our current data show a dramatic spine loss at this time point (Ghosh et al. 2010). Thus, the synaptic reorganization could enable the HL cortex to rewire and participate in new functions, for example, forelimb functions, after a loss of its original target. This speculation is further strengthened by our observation that spine loss is attenuated in the rostral rim of the HL field, which is in close proximity to the intact forelimb.

In hippocampal pyramidal neurons, the synapses proximal to the soma receive local inputs, whereas the distant inputs project to the more distal spines (Spruston 2008). Whether the local–distal input segregation is also true for the sensory-motor cortex is not known, but under the assumption that this is a general feature of the cortex, the preservation of distal spines after thoracic spinal cord injury may allow the injured hind limb cortical neurons to maintain or form new connections with distant functional circuits—for instance, with the forelimb area. On the other hand, the lost proximal spines may reflect disconnection from the dysfunctional neighborhood.

Here, we have documented that spine loss occurs on the apical dendrite of axotomized and with a slower time course also of non-axotomized layer 5b neurons in the denervated HL cortex after spinal cord injury. The reduced spine density after axonal injury probably results in cortical circuits with diminished connectivity. These changes and the synapses that remain may play a critical role in the functional reorganization of the adult cortex after spinal cord injury.

Supplementary Material

Supplementary material can be found at: http://www.cercor.oxfordjournals.org/.

Funding

Swiss National Science Foundation (Grants 31-63633.00 and 31-122527); the National Center of Competence in Research "Neural Plasticity and Repair" of the Swiss National Science Foundation; the Spinal Cord Consortium of the Christopher Reeve Paralysis Foundation (Springfield, NJ); and NeuroNe, Network of Excellence of the European Consortium for Research in Neurodegenerative Diseases (Sixth Framework European Union Program). Investigator A.G. is supported by a Society in Science Branco Weiss Fellowship.

Notes

We thank the microscopy centre at the University of Zurich (ZMB), Ms Anne Greet Bittermann, Mrs Franziska Christ, Ms Eva Hochreutener, and Ms Mirijam Gullo for their technical assistance. *Conflict of Interest* : None declared.

References

Akintunde A, Buxton DF. 1992. Origins and collateralization of corticospinal, corticopontine, corticorubral and corticostriatal tracts: a multiple retrograde fluorescent tracing study. Brain Res. 586:208–218.

Asanuma H, Arissian K. 1982. Motor deficit following interruption of sensory inputs to the motor cortex of the monkey. Electroencephalogr Clin Neurophysiol Suppl. 36:415–421.

Ayling OG, Harrison TC, Boyd JD, Goroshkov A, Murphy TH. 2009. Automated light-based mapping of motor cortex by photoactivation of channelrhodopsin-2 transgenic mice. Nat Methods. 6:219–224.

Bareyre FM, Kerschensteiner M, Raineteau O, Mettenleiter TC, Weinmann O, Schwab ME. 2004. The injured spinal cord spontaneously forms a new intraspinal circuit in adult rats. Nat Neurosci. 7:269–277.

Barron KD, Dentinger MP, Popp AJ, Mankes R. 1988. Neurons of layer Vb of rat sensorimotor cortex atrophy but do not die after thoracic cord transection. J Neuropathol Exp Neurol. 47:62–74.

Brosamle C, Schwab ME. 1997. Cells of origin, course, and termination patterns of the ventral, uncrossed component of the mature rat corticospinal tract. J Comp Neurol. 386:293–303.

Brown CE, Aminoltejari K, Erb H, Winship IR, Murphy TH. 2009. In vivo voltage-sensitive dye imaging in adult mice reveals that somatosensory maps lost to stroke are replaced over weeks by new structural and functional circuits with prolonged modes of activation within both the peri-infarct zone and distant sites. J Neurosci. 29:1719–1734.

Carter LM, Starkey ML, Akrimi SF, Davies M, McMahon SB, Bradbury EJ. 2008. The yellow fluorescent protein (YFP-H) mouse reveals neuroprotection as a novel mechanism underlying chondroitinase ABC-mediated repair after spinal cord injury. J Neurosci. 28:14107–14120.

Catsman-Berrevoets CE, Lemon RN, Verburgh CA, Bentivoglio M, Kuypers HG. 1980. Absence of callosal collaterals derived from rat corticospinal neurons. A study using fluorescent retrograde tracing and electrophysiological techniques. Exp Brain Res. 39:433–440.

Doster SK, Lozano AM, Aguayo AJ, Willard MB. 1991. Expression of the growth-associated protein GAP-43 in adult rat retinal ganglion cells following axon injury. Neuron. 6:635–647.

Feng G, Mellor RH, Bernstein M, Keller-Peck C, Nguyen QT, Wallace M, Nerbonne JM, Lichtman JW, Sanes JR. 2000. Imaging neuronal subsets in transgenic mice expressing multiple spectral variants of GFP. Neuron. 28:41–51.

Fiala JC, Spacek J, Harris KM. 2002. Dendritic spine pathology: cause or consequence of neurological disorders? Brain Res Brain Res Rev. 39:29–54.

Fouad K, Pedersen V, Schwab ME, Brosamle C. 2001. Cervical sprouting of corticospinal fibers after thoracic spinal cord injury accompanies shifts in evoked motor responses. Curr Biol. 11:1766–1770.

Ganchrow D, Bernstein JJ. 1981. Bouton renewal patterns in rat hindlimb cortex after thoracic dorsal funicular lesions. J Neurosci Res. 6:525–537.

Ghosh A, Haiss F, Sydekum E, Schneider R, Gullo M, Wyss MT, Mueggler T, Baltes C, Rudin M, Weber B, et al. 2010. Rewiring of hindlimb corticospinal neurons after spinal cord injury. Nat Neurosci. 13:97–104.

Ghosh A, Sydekum E, Haiss F, Peduzzi S, Zorner B, Schneider R, Baltes C, Rudin M, Weber B, Schwab ME. 2009. Functional and anatomical reorganization of the sensory-motor cortex after incomplete spinal cord injury in adult rats. J Neurosci. 29:12210–12219.

Globus A, Rosenzweig MR, Bennett EL, Diamond MC. 1973. Effects of differential experience on dendritic spine counts in rat cerebral cortex. J Comp Physiol Psychol. 82:175–181.

Haase P, Payne JN. 1990. Comparison of the efficiencies of true blue and diamidino yellow as retrograde tracers in the peripheral motor system. J Neurosci Methods. 35:175–183.

Hains BC, Black JA, Waxman SG. 2003. Primary cortical motor neurons undergo apoptosis after axotomizing spinal cord injury. J Comp Neurol. 462:328–341.

Hubener M, Bolz J. 1988. Morphology of identified projection neurons in layer 5 of rat visual cortex. Neurosci Lett. 94:76–81.

Kaas JH, Qi HX, Burish MJ, Gharbawie OA, Onifer SM, Massey JM. 2008. Cortical and subcortical plasticity in the brains of humans, primates, and rats after damage to sensory afferents in the dorsal columns of the spinal cord. Exp Neurol. 209:407–416.

Kaneko T, Cho R, Li Y, Nomura S, Mizuno N. 2000. Predominant information transfer from layer III pyramidal neurons to corticospinal neurons. J Comp Neurol. 423:52–65.
Keck T, Mrsic-Flogel TD, Vaz Afonso M, Eysel UT, Bonhoeffer T, Hubener M. 2008. Massive restructuring of neuronal circuits during functional reorganization of adult visual cortex. Nat Neurosci. 11:1162–1167.
Kim BG, Dai HN, McAtee M, Vicini S, Bregman BS. 2006. Remodeling of synaptic structures in the motor cortex following spinal cord injury. Exp Neurol. 198:401–415.
Kossut M. 1998. Experience-dependent changes in function and anatomy of adult barrel cortex. Exp Brain Res. 123:110–116.
McComas AJ, Wilson P. 1968. An investigation of pyramidal tract cells in the somatosensory cortex of the rat. J Physiol. 194:271–288.
Merline M, Kalil K. 1990. Cell death of corticospinal neurons is induced by axotomy before but not after innervation of spinal targets. J Comp Neurol. 296:506–516.
Nielson JL, Sears-Kraxberger I, Strong MK, Wong JK, Willenberg R, Steward O. 2010. Unexpected survival of neurons of origin of the pyramidal tract after spinal cord injury. J Neurosci. 30:11516–11528.
Spruston N. 2008. Pyramidal neurons: dendritic structure and synaptic integration. Nat Rev Neurosci. 9:206–221.
Starkey ML, Barritt AW, Yip PK, Davies M, Hamers FP, McMahon SB, Bradbury EJ. 2005. Assessing behavioural function following a pyramidotomy lesion of the corticospinal tract in adult mice. Exp Neurol. 195:524–539.
Trachtenberg JT, Chen BE, Knott GW, Feng G, Sanes JR, Welker E, Svoboda K. 2002. Long-term in vivo imaging of experience-dependent synaptic plasticity in adult cortex. Nature. 420:788–794.
Tseng GF, Prince DA. 1996. Structural and functional alterations in rat corticospinal neurons after axotomy. J Neurophysiol. 75:248–267.
Wannier T, Schmidlin E, Bloch J, Rouiller EM. 2005. A unilateral section of the corticospinal tract at cervical level in primate does not lead to measurable cell loss in motor cortex. J Neurotrauma. 22:703–717.
Wu MM, Fan DG, Tadmori I, Yang H, Furman M, Jiao XY, Young W, Sun D, You SW. 2010. Death of axotomized retinal ganglion cells delayed after intraoptic nerve transplantation of olfactory ensheathing cells in adult rats. Cell Transplant. 19:159–166.
Yuste R, Bonhoeffer T. 2001. Morphological changes in dendritic spines associated with long-term synaptic plasticity. Annu Rev Neurosci. 24:1071–1089.